Optimization of the Hot Forging Processing Parameters for Powder Metallurgy Fe-Cu-C Connecting Rods Based on Finite Element Simulation

FENGXIAN LI, JIANHONG YI, and JÜRGEN ECKERT

Powder forged connecting rods have the problem of non-uniform density distributions because of their complex geometric shape. The densification behaviors of powder metallurgy (PM) connecting rod preforms during hot forging processes play a significant role in optimizing the connecting rod quality. The deformation behaviors of a connecting rod preform, a Fe-3Cu-0.5C (wt pct) alloy compacted and sintered by the powder metallurgy route (PM Fe-Cu-C), were investigated using the finite element method, while damage and friction behaviors of the material were considered in the complicated forging process. The calculated results agree well with the experimental results. The relationship between the processing parameters of hot forging and the relative density of the connecting rod was revealed. The results showed that the relative density of the hot forged connecting rod at the central shank changed significantly compared with the relative density at the big end and at the small end. Moreover, the relative density of the connecting rod was sensitive to the processing parameters such as the forging velocity and the initial density of the preform. The optimum forging processing parameters were determined and presented by using an orthogonal design method. This work suggests that the processing parameters can be optimized to prepare a connecting rod with uniform density distribution and can help to better meet the requirements of the connecting rod industry.

I. INTRODUCTION

POWDER metallurgy (PM) is a promising approach to reduce production costs and improve material performance. Powder forging connecting rod technology combines the advantages of PM and precision forging in a single operation. It also provides a method of manufacturing connecting rod resulting in materials savings, and it directly prepares a near-net-shaped connecting rod with uniform density distribution and excellent mechanical properties from the sintered preform.

Powder forged connecting rods not only have a non-uniform cross-section (*i.e.*, the small end and the big end are thick compared with the central shank), but also have a complex geometric shape, as shown in Figure 1.

During the powder forging connecting rod process, a connecting rod preform with a relative density of 0.7 to 0.8, fabricated by the conventional PM process, needs to be hot forged to its final shape with substantial densification.[1] Unfortunately, powder forged connecting rods always have challenges with poor controllability in metal flow behavior during the forming process and non-uniform density distribution. By controlling the process properly during hot forging, it is possible to control hot forging yield in the manufacturing of connecting rod with high density and excellent mechanical properties.

Inspection of the available literature demonstrates that the densification behaviors of PM materials have been under great development. Some of the previous works treated the PM materials as fully dense materials, while others focused on porosity elimination of the sintered compact only considering a simple geometry.[2–4] In powder forging connecting rods, the yield function for compressible PM materials is different from that of fully dense materials. Moreover, the complex geometric shape of the connecting rod and the relative density of the connecting preform are important factors in governing the connecting rod quality, and thus, they should be considered. The dynamics of the hot forging

FENGXIAN LI and JIANHONG YI are with Kunming University of Science and Technology, Kunming 650093, China. Contact e-mail: clfxl@scut.edu.cn, clfxl@kmust.edu.cn JÜRGEN ECKERT is with Erich Schmid Institute of Materials Science, Leoben 8700, Austria.

process presents a significant challenge for the development of meaningful models. A.D. Abdullin et al. simulated the casting and metal-forming operations with finite element method (FEM) software.[5] J.W. Qiu et al. established a constitutive equation for PM titanium alloy using isothermal compression tests and simulated the hot forming process with FEM software.[6,7] A. Rajeshkannan et al. studied the microstructures and mechanical properties of connecting rod made by powder forging process.[8] Interestingly, FEM used for mechanical behavior simulation offers the possibility to a reduction of the cost and time effectively in the optimization of processing parameters and tool design. However, in many cases, it has not been fully understood how to minimize the porosity by identifying and controlling the main parameters during hot forging.

Moreover, it is evident that the damage and friction behaviors of the PM connecting rod preform during hot forging are important factors in governing its final quality, and should be included in the calculations. The development of ductile damage models has continuously progressed over the last few decades. T.S. Cao successfully modeled cracks' growth under different stress states with the element removal technique.[9,10] R. El Khaoulani et al. obtained a cup-cone fracture in an axisymmetric tensile test.[11] Y. Li et al. predicted fracture limit in the sheet metal forming (S4R in ABAQUS/Explicit).[12] By comparing different criteria, it is clear that the Cockcroft–Latham criterion can give satisfied results for complex stress state applications and was utilized in our work.

In our previous work, the plastic properties of the PM Fe-Cu-C alloy were obtained by isothermal compression tests.[13] Following on from our previous work, the effect of processing parameters on the deformation behaviors of a connecting rod preform during hot forging was investigated using FEM, while damage and friction behaviors of the material were considered in the complicated forging process. The optimum processing parameters were determined and presented by using an orthogonal design method. This article provides insight into manipulating and optimizing the metal flow behavior and improving density of the connecting rod and can help to better meet the requirements of the connecting rod industry.

II. EXPERIMENTAL METHODS AND CALCULATION

A. Plasticity Theory for Porous Metals

For a PM material during the hot forging process, a volumetric strain results in a density change, the Shima and Oyane theory was selected to describe the yield criterion and stress–strain relationship for porous solids:[14]

$$\bar{\sigma} = \frac{1}{\hbar}\left[\frac{(\sigma_1 - \sigma_2)^2 + (\sigma_2 - \sigma_3)^2 + (\sigma_3 - \sigma_1)^2}{2} + \left(\frac{P}{\hat{\lambda}}\right)^2\right]^{1/2},$$

[1]

$$d\varepsilon_i = \frac{3}{2}\frac{1}{\rho_c^{2\lambda-1}}\frac{d\bar{\varepsilon}}{\bar{\sigma}}\left\{\sigma_i - \left(1 - \frac{2}{9\hat{\lambda}^2}\right)P\right\} \quad \text{for } i = 1, 2, 3,$$

[2]

$$d\bar{\varepsilon} = \rho_c^{(\lambda-1)}\left[\frac{2}{9}\left((d\varepsilon_1 - d\varepsilon_2)^2 + (d\varepsilon_2 - d\varepsilon_3)^2 + (d\varepsilon_3 - d\varepsilon_1)^2\right) + (\hat{\lambda}d\varepsilon_v)^2\right]^{1/2},$$

[3]

$$d\varepsilon_v = d\varepsilon_1 + d\varepsilon_2 + d\varepsilon_3,$$

[4]

where $\bar{\sigma}$ and $\bar{\varepsilon}$ refer to the effective stress and the cumulative effective strain, respectively, P is the hydrostatic stress, ρ_c is the relative density, $\hbar$ is a material-dependent factor, and $\hat{\lambda}$ is the ratio between the apparent stress applied to the porous solid and the effective stress exerted on the metal matrix. For sintered porous metals, the factors of $\hbar$ and $\hat{\lambda}$ can be determined as[14]

$$\hat{\lambda} = \frac{1}{\alpha(1 - \rho_c)^\beta}, \quad \hbar = \rho_c^\lambda,$$

[5]

where α, β, and γ are material constants, can be determined from simple compression and tension tests at the tool–work–piece interfaces. It was reported that α, β, and γ were determined as 2.5, 0.51, and 2.5 from experimental results on sintered copper, and confirmed that they are also applicable to sintered iron.[14] This suggests that these material constants are appropriate for the sintered PM Fe-Cu-C alloy in our work.

The relative density can be written as

$$\left(\frac{Q}{\sigma'_m}\right)^2 + 2.5^2(1 - \rho_c)^{1.028}\left(\frac{P}{\sigma'_m}\right)^2 - \rho_c^5 = 0,$$

[6]

where Q is the von Mises equivalent stress, σ'_m is the matrix yield stress.

The plastic property of the PM Fe-Cu-C alloy was obtained from our previous work. And the constitutive equation of PM Fe-Cu-C alloy was obtained as follows:[13]

$$\varepsilon = 5 \times 10^7[\sinh(0.01\sigma)]^{5.93}\exp[-188,420/(8.314T)].$$
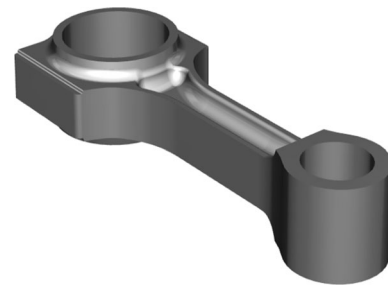
[7]

Fig. 1—Schematic of the connecting rod.

In DEFORM-3D software, damage specifies the damage factor at each element. The damage factor C_d describes the probability of damage. The larger the damage factor, the higher the probability of damage. In our work, the Cockroft–Latham criterion was utilized:[16]

$$\int \frac{\sigma_{max}}{\bar{\sigma}} d\bar{\varepsilon} = C_d, \qquad [8]$$

where σ_{max} is the tensile maximum principal stress, $d\bar{\varepsilon}$ is the effective strain increment. Fracture occurs when the damage factor has reached its critical value. The critical value of the damage factor, C_0, can be determined through physical experimentation.

The plastic flow in PM materials as they undergo hot forging processes can be simulated by using the FEM. For finite element discretization, the duality of the boundary value problem and the variation problem can be described as[17]

$$\delta\pi = \int_v \bar{\sigma} \delta\dot{\bar{\varepsilon}} dV + K \int_v \dot{\varepsilon}_v \delta\dot{\varepsilon}_v dV - \int_{S_F} F_i \delta u_i dS = 0, \quad [9]$$

where π is a function of the total energy and work; $\dot{\bar{\varepsilon}}$ the effective strain rate; F_i represents the surface tractions; u_i is the velocity component; $\delta\dot{\bar{\varepsilon}}$ and $\delta\dot{\varepsilon}_v$ are the variations in strain rate and volumetric strain rate, respectively; and K is a penalty constant having a very large positive value. For a detailed description of the finite element theory and the modeling formulations, readers are referred to Reference 18.

B. Cooling Behavior of the PM Connecting Rod Preform During Forging

The solidification behavior of the PM connecting rod preform during forging is a thermo-mechanical process. The equations governing thermo-mechanical deformation are summarized as[19]

$$Q_I + A\left(\frac{\partial^2 T}{\partial x^2} + \frac{\partial^2 T}{\partial y^2} + \frac{\partial^2 T}{\partial z^2}\right) - \rho C \frac{\partial T}{\partial t} = 0, \qquad [10]$$

where A is the thermal conductivity and Q_I is the heat generation term representing the heat released due to plastic work, and can be calculated using Eq. [11]:

$$Q_I = B \cdot \bar{\sigma} \cdot \bar{\varepsilon}, \qquad [11]$$

where B is the efficiency of conversion of plastic work into heat, and assumed to be about 0.9 for PM Fe-Cu-C alloy.

For the inter stand cooling, heat loss is calculated as

$$Q_1 = h_1(T - T_a) + \omega\xi(T^4 - T_a^4), \qquad [12]$$

where T_a is the ambient temperature, ω is the constant emissivity of the preform surface, and ξ is the Stefan–Boltzmann constant.

Contact heat loss model used is expressed as

$$Q_2 = h_2(T - T_a), \qquad [13]$$

where h_2 is the convection coefficient at the preform/model interface. Interfacial contact during hot forging of PM Fe-Cu-C alloy is similar to that during hot deformation of Fe-Cu-C alloy. Thus, the interfacial heat transfer coefficient during hot forging of PM Fe-Cu-C alloy is comparable with that during hot deformation of Fe-Cu-C alloy. Consequently, the convection coefficients, h_1 and h_2, were determined as 28 and 4.8×10^4 W m^{-2} K^{-1}, respectively.[20,21]

The friction heat Q_3 between preform and model is written as

$$Q_3 = C \cdot |\tau \cdot \Delta v|, \qquad [14]$$

where τ is the friction force, Δv is the preform–model relative velocity, and C is the distribution coefficient of heat.

C. Numerical Implementation

A general purpose, proprietary finite element software program, DEFORM-3D, has been used to simulate the deformation processes occurring during the hot forging of PM connecting rod preform. For the convenience of model establishment, some assumptions are made in the model as follows: the models are considered as rigid material while the elastic deformation ignored. Since the initial density of the connecting rod preform is affected by the PM process, for simplicity, the average density of the preform is selected as an initial preform density in the present simulation. Then, generic algorithms of coupling of temperature field and strain field were developed according to these assumptions. Three-dimensional FEM is used to build the analysis model, as shown in Figure 2.

The definition of the element mesh used isoperimetric four-node elements foresees the discretization of the sintered materials and the mold, as well as the schematization of the contact between the bodies. The connecting rod preform is divided into 75,682 elements and 18,624 nodes, as shown in Table I.

The setting of the mesh density in the deformation zones was varied according to the strain or strain-rate distributions. An adaptive mesh is utilized which can drastically reduce the total processing time. The
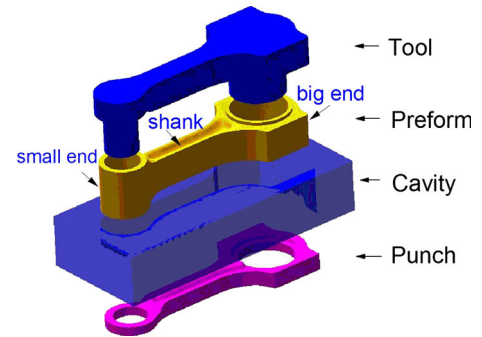

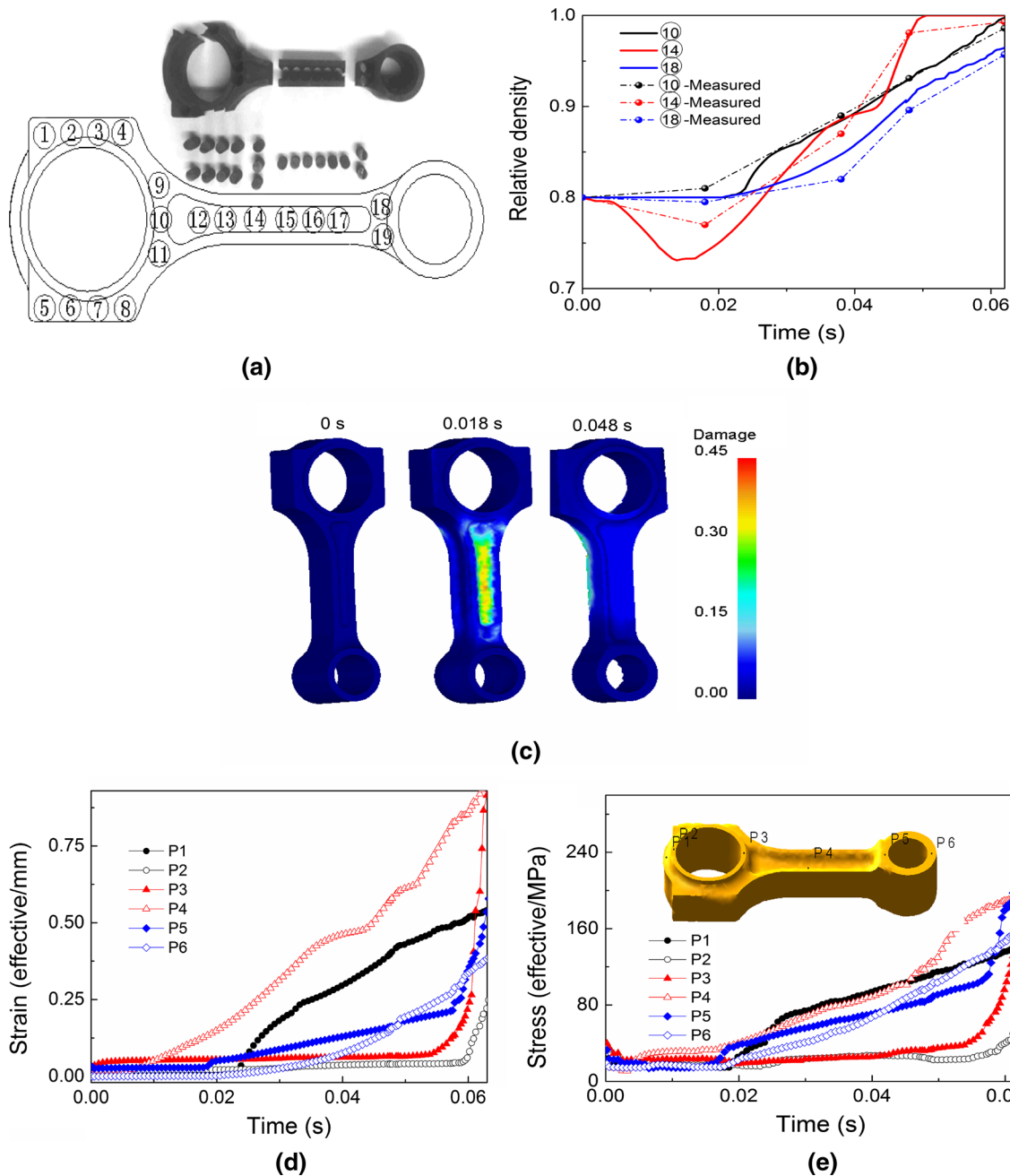Fig. 2—Geometrical model assembly of tool, punch, preform, and cavity.

Fig. 3—The comparisons of (a) and (b) relative density and (c) damage distribution of the connecting rod after forging between the simulated and experimental results, and calculated (d) effective strain and (e) effective stress distributions at various forging times.

Table I. The Element Numbers and Nodes of Three-Dimensional Mesh

	Preform	Top Die	Cavity Block	Bottom Die
Elements	75,682	76,559	64,899	14,521
Nodes	18,642	18,024	15,468	61,235

calculation is carried out in simulation engine which can handle the types of preform (porous material) and dies (rigid) with non-isothermal simulation capability. An updated Lagrange procedure was used to account for large strain plasticity, with enthalpy and temperature at each mesh node conservatively transferred onto the new mesh in the next time step. The simulation results can be accessed through the post.

During the hot forging process, thermo-physical property data of PM Fe-Cu-C alloy and H13 were

Table II.   Physical Properties of PM Fe-Cu-C Alloy[22,23]

Elastic modulus	155
Poisson's ratio	0.28
Tensile strength (MPa)	460
Heat capacities per unit mass (J kg^{-1} K^{-1})	$C_p = 317.202 + 0.433 \times T$

Table III.   Physical Properties of H13 Die[22,23]

Temperature	293 K (20 °C)	573 K (300 °C)	773 K (500 °C)
Elastic modulus (10^{11} Pa)	2.10	1.91	1.75
Thermal conductivity (W m^{-1} K^{-1})	36.6	32.1	29.7
Heat capacities per unit mass (J kg^{-1} K^{-1})	445.6	553	641

Table IV.   Comparison of the Calculated Results and Experimental Results

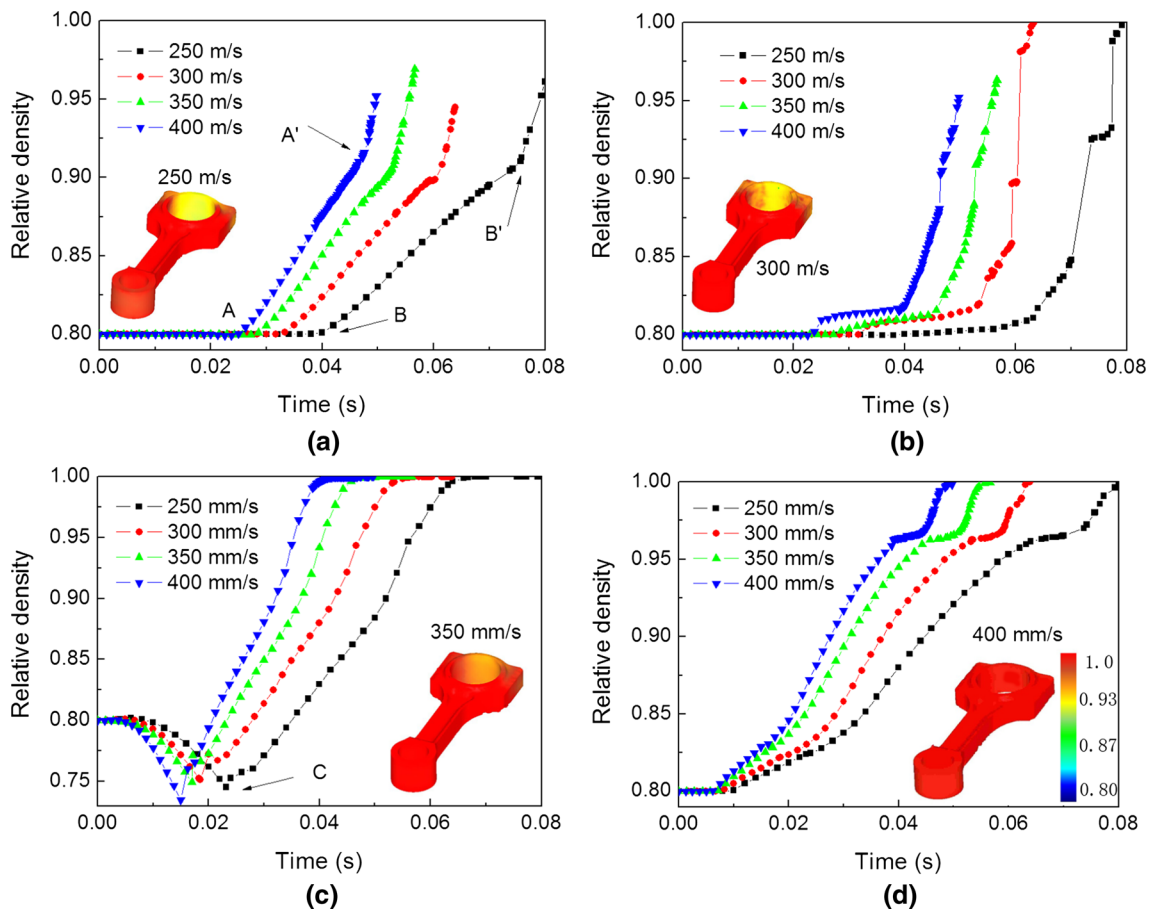|	P1	P4	P5	P8	P10	P14	P17	P18	P19
Calculated $\rho_{c\text{-}1}$	0.998	1.000	0.995	0.992	0.991	0.995	0.994	0.966	0.946
Experimental $\rho_{e\text{-}1}$	0.986	0.991	0.988	0.989	0.986	0.993	0.973	0.957	0.955
Calculated $\rho_{c\text{-}2}$	0.981	0.976	0.978	0.965	0.928	0.972	0.971	0.914	0.921
Experimental $\rho_{e\text{-}2}$	0.969	0.965	0.980	0.976	0.931	0.981	0.982	0.896	0.894

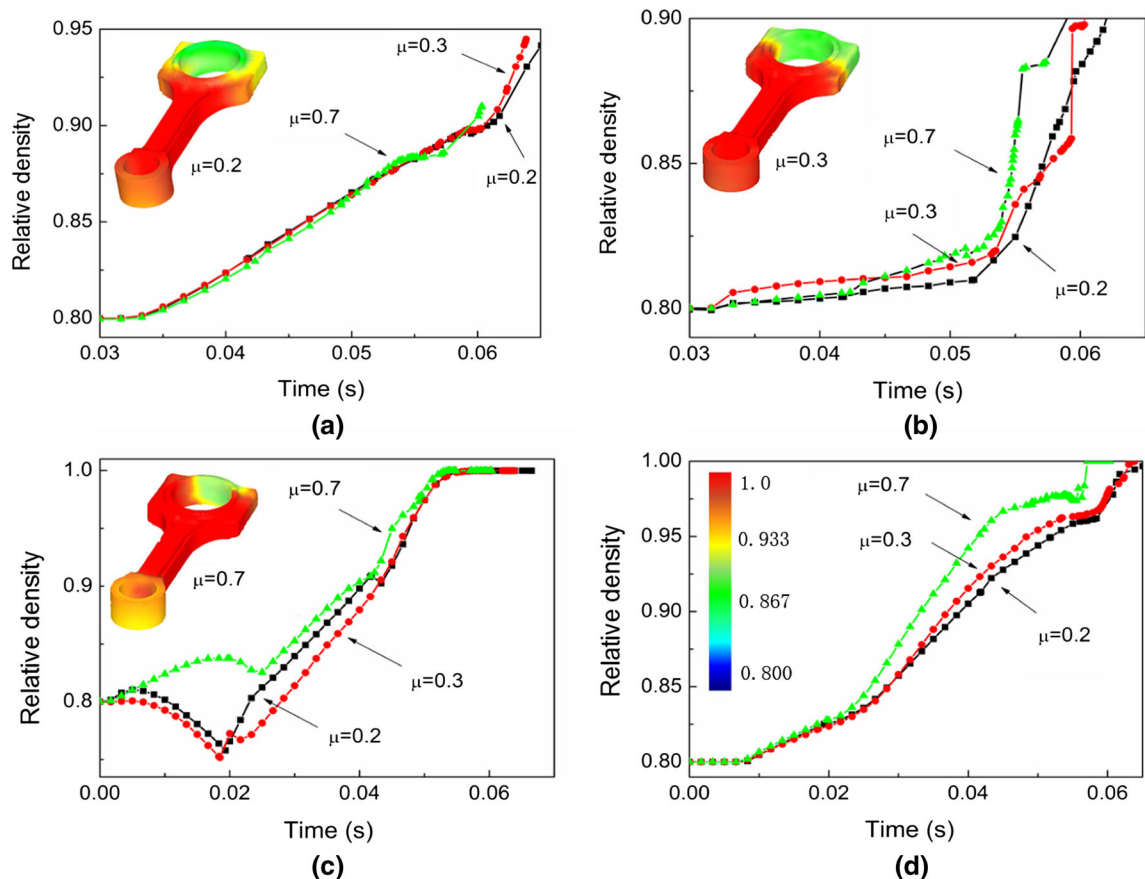Fig. 4—Relative density distributions at various forging velocities: (*a*) P1, (*b*) P2, (*c*) P4, and (*d*) P6.

Fig. 5—Relative density distributions at various friction factors: (*a*) P1, (*b*) P2, (*c*) P4, and (*d*) P6.

obtained from the publications provided by Battle, and are listed in Tables II and III.[22,23] The ring test can be used for evaluating friction in forging of fully dense materials and can also be applied to powder forging.[15,19,24] For hot forging of PM Fe-Cu-C alloy with a relative density of 0.7 to 0.8, the friction factors can be determined as 0.3 based on the reported results.

D. *Experimental Method*

During the powder forging connecting rod process, a connecting rod preform fabricated by the conventional PM route with a relative density of 0.7 to 0.8 was selected as the material.

First, four connecting rod preforms were hot forged in a closed die with a forging velocity of 250 mm s^{-1}, a friction coefficient of 0.3, an initial preform temperature of 1403 K (1130 °C), and a preheated model temperature of 573 K (300 °C). One of the preforms was forged to its final shape. For the other rods, the forging process was stopped after 0.018, 0.038, and 0.048 seconds when the preform had been partially deformed. Samples with a diameter of 8 mm and a height of 12 mm were cut at various axial locations. The apparent density of the samples can be measured with a buoyancy weighing machine. Second, in order to verify the validity of optimized processing parameters, the hot forging experiment was carried out under the optimized processing

parameters. Samples were cut from the connecting rod preform at various axial locations. Then the densities were measured.

In accordance with experimental data and based on the established models, we can investigate the effects of the processing parameters on the density profiles of the connecting rod. Variations of process parameters have also been made with respect to time. These variations will be discussed in the following section.

III. RESULTS AND DISCUSSION

A. *Verification of Numerical Simulation Results*

For densification of the connecting rod preform in a closed die with a forging velocity of 250 mm s^{-1}, a friction coefficient of 0.3, an initial preform temperature of 1403 K (1130 °C), and a preheated mold temperature of 573 K (300 °C), the measured and calculated relative densities at various axial locations are compared, as shown in Figures 3(a) and (b) and Table IV. The calculated values of ρ_{c-1} at P10 (at the big end) and at P18 (at the small end) of the connecting rod at the conclusion of the hot forging process are 0.991 and 0.966, respectively, which closely match the measured values of ρ_{e-1} 0.986 and 0.957 produced by experiments at the corresponding locations. Furthermore, the
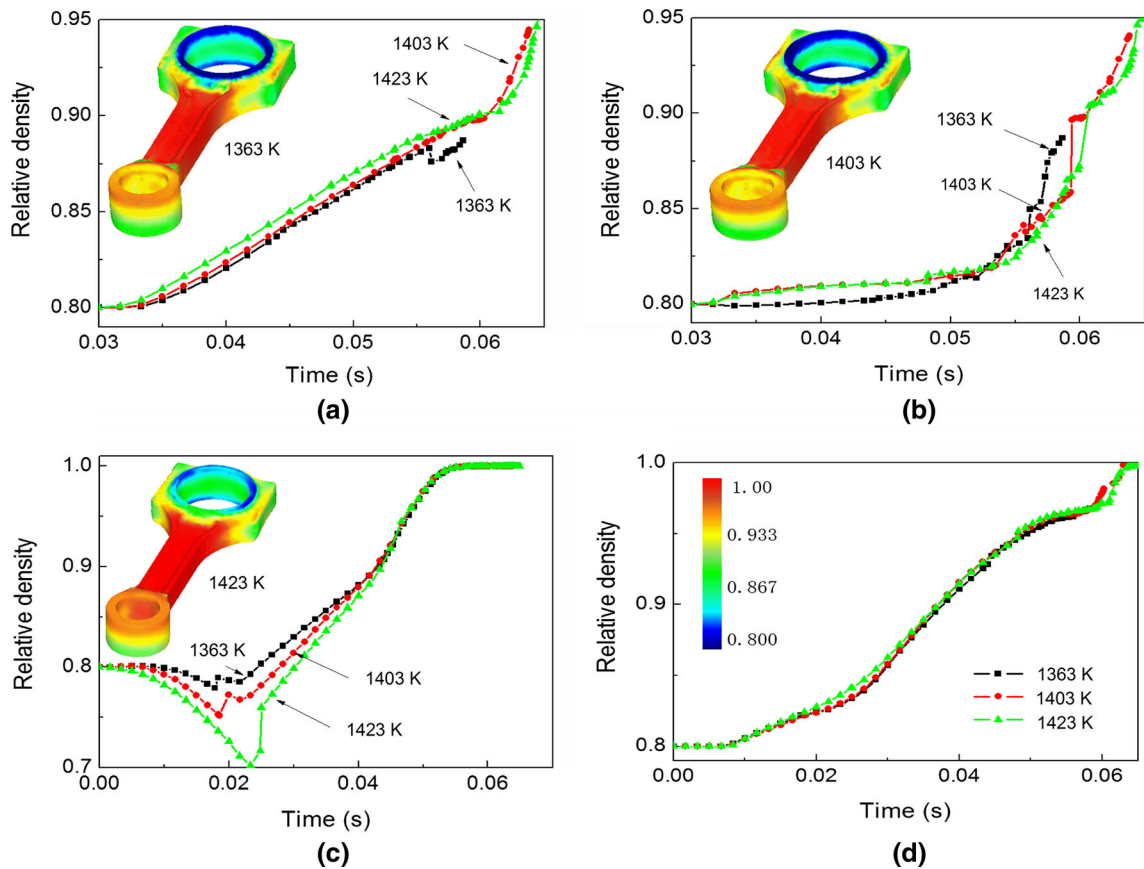
Fig. 6—Relative density distributions at various preheating temperatures of preforms: (*a*) P1, (*b*) P2, (*c*) P4, and (*d*) P6.

measured values of the partially deformed connecting rod correspond well with the calculated results. For example, the calculated value of $\rho_{c-2} = 0.914$ at P18 (at the small end) of the rod deformed for 0.048 seconds corresponds well with the measured value of $\rho_{e-2} = 0.896$ at the same location and at the same time. The deviation between the simulated and experimental contours is small. Clearly, the calculated relative density distribution of the connecting rod corresponds well with that produced by experiments.

Moreover, much more attention was paid to the forging process for a duration of around 0.018 seconds, in which the relative density at P14 decreased initially and then increased, as shown in Figure 3(b). The damage profiles of the connecting rod during hot forging process, at nearly 0.018 seconds deformation, were estimated and are displayed in the color maps together with those for 0 and 0.048 seconds, as shown in Figure 3(c). The damage factor values of C_d at the shank are 0.32, which are large compared with the damage factors at other positions and other times. This means that the shanks are prone to cracking at this time. This may lead to a decrease of the relative density. However, the fracture does not occur at this moment as C_d has not reached its critical value of $C_0 = 0.45$. Then the crack can be eliminated at 0.048 seconds when this zone is fully deformed. Therefore, the relative density increased continuously. Cracks occurred easily at the shank can also be explained by the variations of effective

strain and effective stress of the connecting rod, as shown in Figures 3(d) and (e). The curves of the effective stress and the effective strain at the shank under the same processing conditions increased dramatically. Namely, large deformations were present. The shanks are prone to cracking because of the higher deformation rates. If this zone is not fully deformed due to inappropriate process parameters, cracking will be exacerbated.

The above analysis can improve that our previous modeling may provide a useful approach to predict the relative density profiles of connecting rod under various processing conditions.

B. *Influence of Processing Parameters on Relative Density Distribution*

The method described above was applied in a series of examples to demonstrate the effect of the processing parameters on the relative density distribution of the connecting rod. According to the experimental conditions, the typical ranges of processing parameters considered in the simulation are as follows: forging velocity ranges from 250 to 400 mm s^{-1}, preheat temperature of preform ranges from 1363 K to 1423 K (1090 °C to 1150 °C), and initial relative density of preform ranges from 0.7 to 0.85. The friction coefficient of the materials is dependent upon the working temperatures. Therefore, friction coefficient ranges from 0.2 to

0.7.[15,19,24] Four representative points were selected to study the different areas of the connecting rod (*i.e.*, P1, P2, P4, and P6), as shown in Figure 3(e), while P1 and P6 are points on the surface at the big end and at the small end, respectively; P2 is a point on the surface of the position at the big end; P4 is a point on the surface of the position at the shank. In this work, the processing parameters corresponding to the high and unique density distribution, especially at P1, P2, P4, and P6, can be considered as suitable candidates for hot working parameters.

1. *Influence of forging velocity*

The forging velocity has a significant influence on the relative density distribution of connecting rod, as shown in Figure 4. When compared with the densification progression at the big end, P1 (Figure 4(a)) and P2 (Figure 4(b)), the densification progressed first at the shank (P4), as shown in Figure 4(c). However, the relative density at P4 decreased initially and then increased. This can be attributed to the fact that P4 was first in contact with the mold, and will cool down by heat transfer to the die, and thus, the temperature of the material at P4 decreases faster. Then cracking unavoidably occurred with the faster cooling rate and at higher deformation rates. However, the crack can be eliminated

when this zone is fully deformed. Therefore, the relative density increased continuously. Moreover, the geometry of the connecting rod preform is an important factor in governing the metal flow behavior of the PM Fe-Cu-C during the hot forging process. Because the shape of the connecting rod preform was not optimized and changed, the relative density of all materials at P4 in this work decreased and then increased. However, once the shape of the preform was optimized, the density of materials at P4 increased with time. Meanwhile, with an increasing forging velocity, the rate of increase of the relative density at P6 is accelerated, as shown in Figure 4(d). As the PM connecting rod preform contained internal void defects, the pores sealed effectively, which lead to increasing densities during the early stages. With increasing metal flow resistance, a higher forging force was required. It can be concluded that the deformation and densification behaviors of the PM Fe-Cu-C alloy occur at the same time during the forging process. When the forging velocity is below 250 mm s^{-1}, the quality was deteriorated (*i.e.*, the big end is hard to achieve complete density).

2. *Influence of friction coefficient*

Figure 5 shows the effect of the friction coefficient on the relative density when other processing parameters
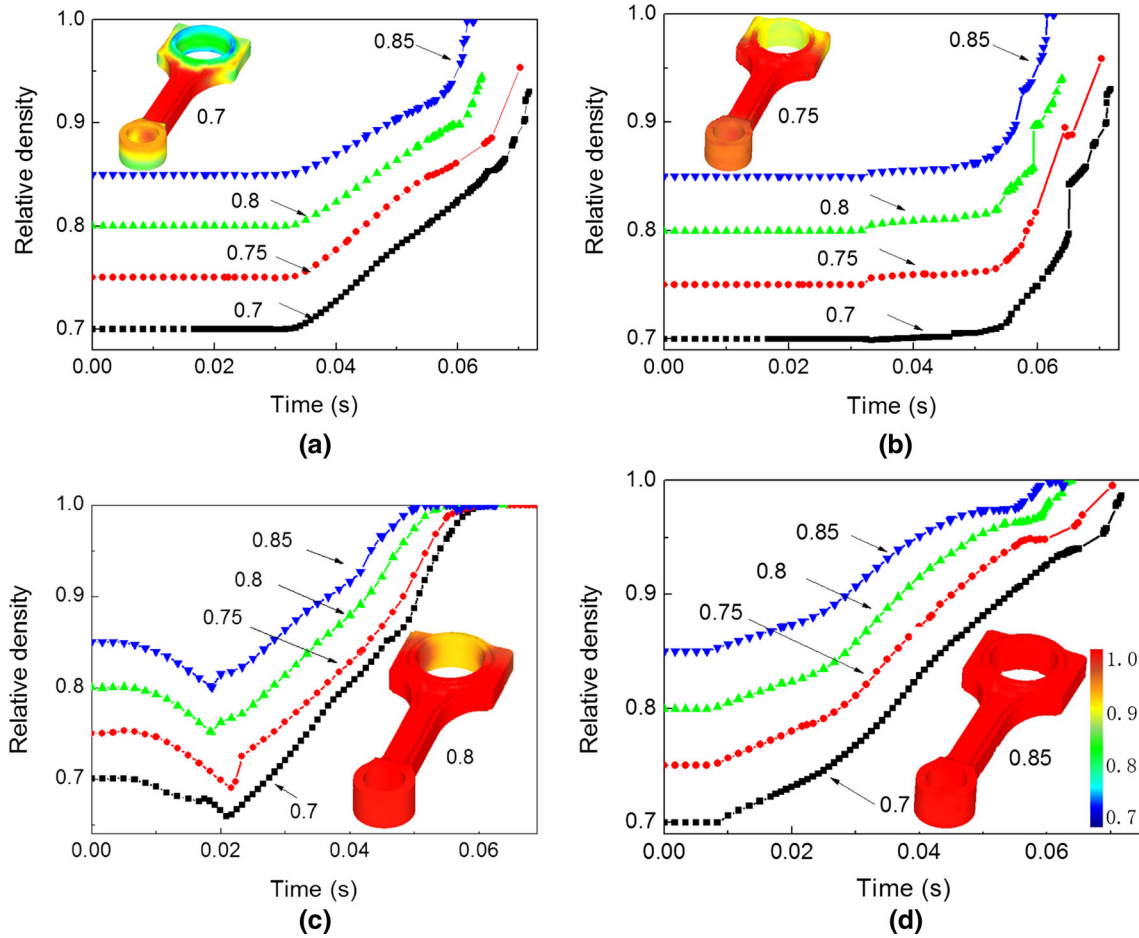

Fig. 7—Relative density distributions at various initial densities of the preforms: (*a*) P1, (*b*) P2, (*c*) P4, and (*d*) P6.

Table V. The Uniform Designs L$_{16}$ (4^5) and the Orthogonal Table of Max Relative Density

Factors	Forging Velocity	Friction Coefficient	Preheating Preforms Temperature	Initial Density of Preforms
Value 1	250 mm s^{-1}	0.2	1363 K (1090 °C)	0.7
Value 2	300 mm s^{-1}	0.3	1403 K (1130 °C)	0.75
Value 3	350 mm s^{-1}	0.3	1403 K (1130 °C)	0.8
Value 4	400 mm s^{-1}	0.7	1423 K (1150 °C)	0.85
Average value 1	93.344	93.146	92.604	92.616
Average value 2	92.042	92.882	93.171	92.978
Average value 3	92.571	**93.898**	**93.35**	93.264
Average value 4	**94.012**	92.811	93.092	**94.812**
F ratio	0.746	1.087	1.97	2.196
Significant				√

Bold values indicate that the initial density of preforms has the most significant effect on the density of connecting rod.
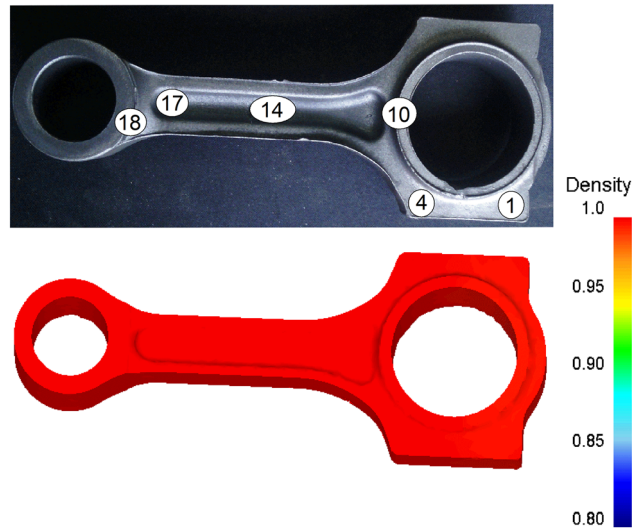

Fig. 8—Hot forged connecting rod and calculated relative density of the connecting rod under the optimized processing parameters.

Table VI. Comparison of the Calculated Results and Experimental Results

	P1	P4	P10	P14	P17	P18
Calculated ρ_c	0.995	0.998	1.000	1.000	0.998	0.998
Experimental ρ_c	0.992	0.994	0.996	0.996	0.996	0.996

are kept constant. By changing the friction coefficient from 0.2 to 0.7, the variation of relative density is not obvious compared with that of forging velocity. Namely, with an increasing friction coefficient, the relative density increases only slightly. During the forging process, the density of the connecting rod at the big end (P1), as shown in Figure 5(a), is lower than the density at small end of the connecting rod (P6) in Figure 5(d). And the relative density at the shank of the connecting rod (P4) in Figure 5(c) shows the same tendency compared with that in Figure 4(c), *i.e.*, the relative density at P4 initially decreased and then increased. However, this zone can be fully deformed and densified at the end of the forging process. Moreover, the relative density at the shank of the connecting rod (P4) shows a slow rise tendency in Figure 5(c) compared with that at the small end of the connecting rod (P6), as shown in Figure 5(d). Generally, more heat will be generated when the friction coefficient increases owing to plastic deformation and the friction at the contact mold/preform surface. Thus, if the temperature drop of the preform surface was alleviated, then materials can be deformed easily, and the relative

density can be increased. It can be concluded that the relative density of the connecting rod in the deformation zone increases with an increasing friction coefficient.

However, an increase of friction coefficient may prohibit the flow ability of the materials. In this case, the good flow ability obtained by a decreasing friction coefficient played a larger role in densification than that by the heat generated at a high friction coefficient. Moreover, a good flow ability of the materials can generate cost savings in the enterprise.

3. Influence of preheating preform temperature
The relative density profiles of the connecting rod for different preheating preform temperatures are illustrated in Figure 6. Higher the preheating temperature of the preform leads to a higher relative density, as shown in Figures 6(a) and (d). In Figure 6(b), the relative density of the connecting rod at P2 for a preheating preform temperature of 1363 K (1090 °C) increases to 0.86 compared with a relative density of 0.80 for a preheating preform temperature of 1423 K (1150 °C). This result is reasonable because high preheating preform temperatures have a high enthalpy in the preform and can lead to a higher deformation temperature.[16] Therefore, the flow ability of materials can be improved. This helps to fill the interstices in materials, which results in porosity elimination. However, the relative density at P4 decreased significantly compared with that at low preheating preform temperatures, as shown in Figure 6(c).

This can be attributed to the fact that increasing preheating preform temperatures lead to a decrease in the deformation resistance of the material. Material at the deformation zone, especially at the shank (P4), had higher deformation rates. If the preheating preform temperature is too high, it will have a negative effect in the surface quality of connecting rod, *i.e.*, oxidation phenomenon of preform. Moreover, it should be taken into consideration

that the wear of molds will be accelerated at high temperatures which should be taken into consideration. In Figure 6, it also appears that the influence of the preheating preform temperature on the relative density is smaller than that of the forging velocity.

4. *Influence of initial density of preform*

Under a different initial density of the preform, the variations in the relative density of the connecting rod at P1, P2, P3, and P4 with time are presented in Figure 7.

It can be seen that the densification progress at the shank (P4) and at the small end (P6) of the connecting rod began much earlier than that at the big end (P1), as shown in Figures 7(a), (c), and (d). The densification at P2 behaved much slower compared with that of any other part but increased with increasing initial density of the preform, as shown in Figure 7(b). Clearly, the influence of the processing parameters on relative density at a high initial preform density is significant compared with that at a low initial preform density, especially at P4, as shown in Figure 7(c). The densification mechanism during the hot forging process corresponds to the removal of the interstitial porosity dominant regime. It can be concluded that the processing parameters can be controlled to minimize porosity, but porosity can be eliminated effectively prior to forging contact. The increments of forging velocity and preheating preform temperature are limited because of the associated increase in capital costs as well as increased energy costs. It is better to control the density of the preform rather than forging. When the initial relative density of the preform is up to 0.8, the connecting rod can achieve full density, as shown in Figure 7(d).

C. *Optimization of Processing Parameters*

The orthogonal design method is always utilized to optimize processing parameters. It is possible to optimize hot forging processing parameters quickly, easily, and accurately by using the uniform design L_{16} (4^5). Four processing parameters with different levels were considered, *i.e.*, the forging velocity, the friction coefficient, the preheating preform temperature, and the initial density of preform. Table V shows the designed and arranged simulation results. The average relative density is sensitive to the processing parameters. The initial preform density plays a significant role on the relative density of the connecting rod in comparison with the other processing parameters. Moreover, the effect of the forging velocity is remarkable compared with the effect of the preheating preform temperature and the friction coefficient. Based on the results of the FEM simulation, the following optimum processing parameters are obtained as follows: the forging velocity is 400 mm s^{-1}, the friction coefficient is 0.3, the preheating preforms temperature is 1403 K (1130 °C), and the initial density of preform is 0.85.

To verify the accuracy of this result, the connecting rod preform was forged experimentally under the optimized processing condition. And the experimental results were compared with the calculated results, as shown in Figure 8. The simulated and measured relative densities at various axial locations, which are the same locations as those in Figure 3(a), are compared in Table VI. For example, the calculated relative density value at P14 at the shank is 1.000, which matches closely with the measured value of 0.996 by experiments. This can demonstrate the processing parameters which can be optimized to prepare a connecting rod with uniform density distribution and can help to better meet the requirements of the connecting rod industry.

This work can present a method, analysis to manipulate the hot forging processing parameters of the connecting rod, and ensure a uniform density distribution and assist to improve the quality of connecting rod.

However, the simulated accuracy should be further improved. As mentioned above, the shape of the connecting rod also has a significant influence on the densification behavior of the preform. Therefore, the optimization of the geometric size of the connecting rod preforms deserves further investigation.

IV. CONCLUSIONS

The densification behaviors of PM connecting rod preforms during hot forging processes were investigated using the FEM. Damage and friction behaviors of the material, a Fe-3Cu-0.5C (wt pct) alloy compacted and sintered by the PM route, were considered in the complicated forging process. The calculated results agree well with the experimental results. The forging velocity and the initial density of preform play significant role on the relative density of the connecting rod in comparison with the other processing parameters, *i.e.*, the friction coefficient and the preheating preform temperature. In general, the relative density of preform during hot forging increases with the increase of the initial density of preform, the forging velocity, the friction coefficient, and the preheating preform temperature. The optimum forging processing parameters were determined and presented by using an orthogonal design method. The present theoretical and experimental analyses suggest that hot forging processing parameters can be optimized to manufacture directly connecting rod with a high density from sintered preform within one step.

REFERENCES

1. R.M. German: *Powder Metallurgy of Iron and Steel*, Wiley, New York, 1998, pp. 276–79.
2. F.X. Li, Y.Z. Liu, J. You, and X. Luo: *Int. J. Adv. Manuf. Technol.*, 2013, vol. 67, pp. 2771–78.
3. F.X. Li and Y.Z. Liu: *Trans. Nonferr. Met. Soc.*, 2013, vol. 24, pp. 2475–81.

4. O. Moriya, S. Susumu, and O. Kunio: *J. Jpn. Soc. Technol. Plast.*, 1979, vol. 20, pp. 21037–44.
5. A.D. Abdullin and A.A. Ershov: *Metallurgist*, 2014, vol. 58, pp. 339–45.
6. J.W. Qiu, Y. Liu, B. Liu, Y.B. Liu, B. Wang, E. Ryba, and H.P. Tang: *J. Mater. Sci.*, 2012, vol. 47, pp. 3837–48.
7. J.W. Qiu, Y. Liu, Y.B. Liu, B. Liu, B. Wang, E. Ryba, and H.P. Tang: *Mater. Des.*, 2012, vol. 33, pp. 213–19.
8. A. Rajeshkannan, K.S. Pandey, S. Shanmugam, and R. Narayanasamy: *Mater. Des.*, 2008, vol. 29, pp. 1862–67.
9. T.S. Cao: *Int. J. Solids Struct.*, 2014, vol. 51, pp. 2370–81.
10. T.S. Cao: *Int. J. Mater. Form.*, 2017, vol. 10, pp. 139–71.
11. R El Khaoulani and P.O. Bouchard: *Finite Elem. Anal. Des.*, 2012, vol. 59, pp. 1–10.
12. Y. Li, M. Luo, J. Gerlach, and T. Wierzbicki: *J. Mater. Process. Technol.*, 2010, vol. 210, pp. 1858–69.
13. F.X. Li, J.H. Yi, and J. Eckert: *Metall. Mater. Trans. A*, 2017, vol. 48A, pp. 2971–78.
14. S. Shima and M. Oyane: *Int. J. Mech. Sci.*, 1976, vol. 18, pp. 285–91.
15. D.C. Chen and C.F. Chen: *J. Mater. Process. Technol.*, 2007, vol. 190, pp. 130–37.
16. M.G. Cockroft and D.J. Latham: *J. Inst. Met.*, 1968, vol. 96, pp. 33–39.
17. D.C. Chen: *J. Mater. Process. Technol.*, 2006, vol. 180, pp. 193–200.
18. S. Kobayashi, S.I. Oh, and T. Altan: *Metal Forming and the Finite Element Method*, Oxford University Press, New York, 1989.
19. X.T. Li, M.T. Wang, and F.S. Du: *Mater. Sci. Eng.*, 2005, vol. 408A, pp. 33–41.
20. F.X. Li, Y.Z. Liu, and J.H. Yi: *Metall. Mater. Trans. A*, 2014, vol. 45A, pp. 4012–21.
21. H. Grass, C. Krempaszky, and E. Werner: *Comput. Mater. Sci.*, 2006, vol. 36, pp. 480–89.
22. T.P. Battle: *Int. Mater. Rev.*, 1992, vol. 37, p. 569.
23. W.D. Wong-Ángel, L. Téllez-Jurado, J.F. Chávez-Alcalá, E. Chavira-Martínez, and V.F. Verduzco-Cedeño: *Mater. Des.*, 2014, vol. 58, pp. 12–18.
24. E. Honarvar Gheysari, A. Babakhani, and A. Haerian: *Int. J. Automot. Eng.*, 2014, vol. 4, pp. 654–63.